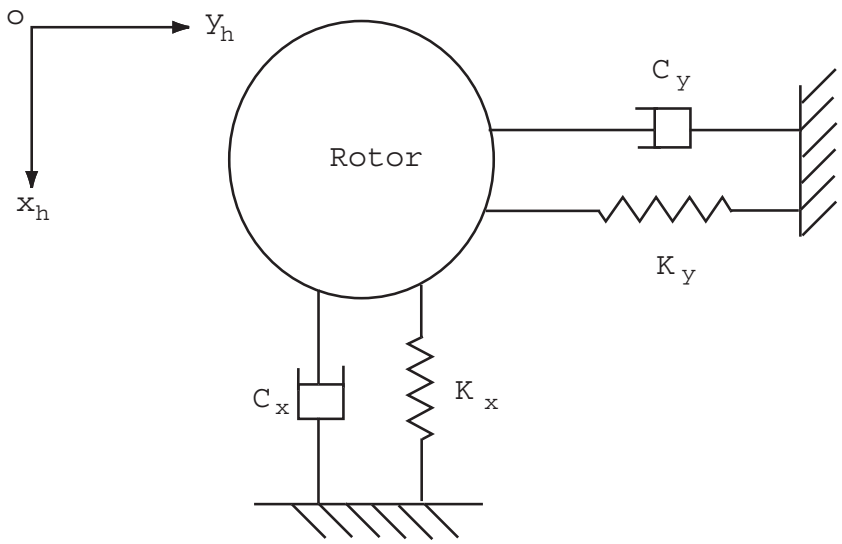

The equations of motion are conveniently expressed in the fixed reference frame. Neglecting the aerodynamic forces, the equations of motion for inplane rotor motion in the fixed frame are

$$\mathrm{I}_\zeta\Omega^2\{(\overset{**}{\zeta}_{lc} + 2\overset{*}{\zeta}_{ls} - \zeta_{lc}) + \nu_\zeta^2\zeta_{lc} + \mathrm{C}_\zeta^*(\overset{*}{\zeta}_{lc} + \zeta_{ls})\} - \mathrm{S}_\zeta\Omega^2\overset{**}{y}_h = 0$$

$$\mathrm{I}_\zeta\Omega^2\{(\overset{**}{\zeta}_{ls} - 2\overset{*}{\zeta}_{lc} - \zeta_{ls}) + \nu_\zeta^2\zeta_{ls} + \mathrm{C}_\zeta^*(\overset{*}{\zeta}_{ls} - \zeta_{lc})\} + \mathrm{S}_\zeta\Omega^2\overset{**}{x}_h = 0$$

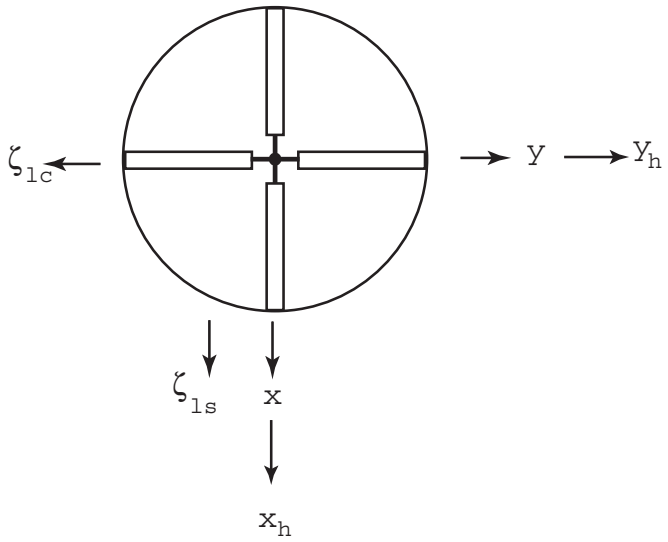

The ν_ζ is the rotating lag frequency and the C_ζ^* is the damping coefficient in the rotating frame due to aerodynamic, structural and mechanical damping. In actuality, the nature of mechanical damping from lag and support dampers is quite nonlinear. For mathematical convenience, these dampings are represented as equivalent viscous dampings and are calculated equating the energies dissipated in one cycle of motion.

$\mathrm{I}_\zeta = \int_e^R r^2\,dm$ mass moment of inertia about lag hinge
$\mathrm{S}_\zeta = \int_e^R r\,dm$ first moment of mass about lag hinge

Let us assume that M_x and M_y the effective masses of body hanging on the springs in the x and y directions respectively. The rotor forces excite the body, and the equations of motion for the body are

$$\mathrm{M}_x\ddot{x}_h + k_x x_h + \mathrm{C}_x\dot{x}_h = H$$

$$\mathrm{M}_y\ddot{y}_h + k_y y_h + \mathrm{C}_y\dot{y}_h = Y$$

The blade inplane forces are

$$\mathrm{S}_r = -2\Omega\dot{\zeta}\int_e^R mr\,dr \; - (\ddot{x}_h\cos\psi + \ddot{y}_h\sin\psi)\int_e^R m\,dr = -2\mathrm{S}_\zeta\,\Omega\dot{\zeta} - \mathrm{M}(\ddot{x}_h\cos\psi + \ddot{y}_h\sin\psi)$$

$$\begin{aligned}\mathrm{S}_x &= -\ddot{\zeta}\int_e^R mr\,dr \; + \Omega^2\zeta\int_e^R mr\,dr - (\ddot{x}_h\sin\psi - \ddot{y}_h\cos\psi)\int_e^R m\,dr \\ &= -\mathrm{S}_\zeta\ddot{\zeta} + \mathrm{S}_\zeta\Omega^2\zeta - \mathrm{M}(\ddot{x}_h\sin\psi - \ddot{y}_h\cos\psi)\end{aligned}$$

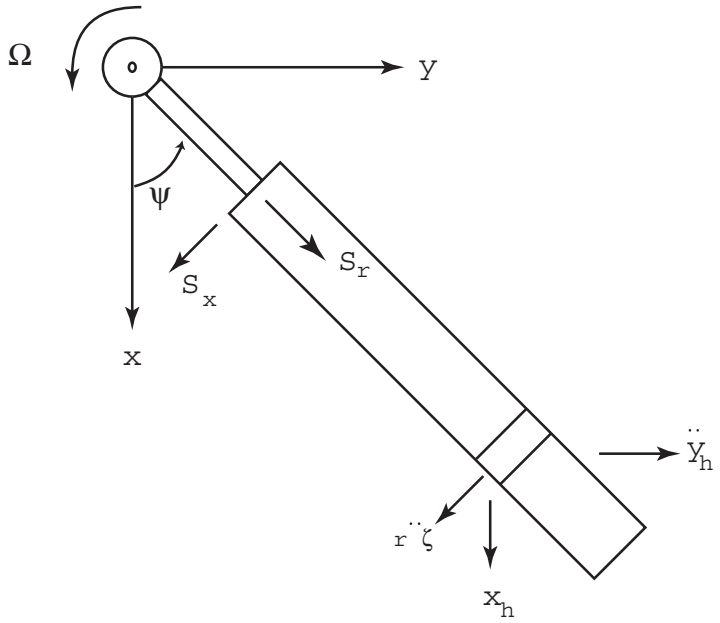

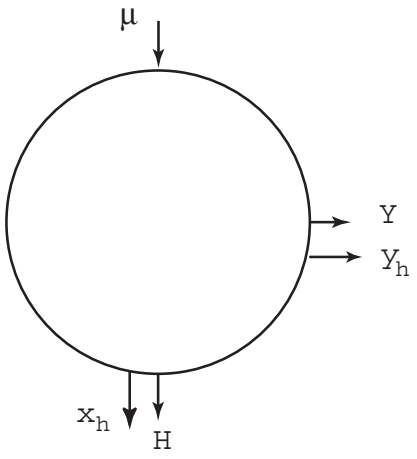

where H and Y are the hub forces due to the rotor and these are expressed as

$$\text{H} = \text{Total resultant drag force} = \sum^{N}(\text{S}_x \sin\psi_m + \text{S}_r \cos\psi_m)$$

$$\begin{aligned}
H &= \sum_{m=1}^{N} \sin\psi_m[-\text{S}_\zeta \ddot{\zeta}^{(m)} + \text{M}\Omega^2\zeta^{(m)} - \text{M}(\ddot{x}\sin\psi_m - \ddot{y}_h\cos\psi_m \\
&\quad + \sum_{m=1}^{N} \cos\psi_m[-2\text{S}_\zeta\Omega\ddot{\zeta}^{(m)} - \text{M}(\ddot{x}_h + \ddot{y}_h\sin\psi_m)] \\
&= -\text{S}_\zeta\Omega^2\frac{N}{2}(\overset{**}{\zeta}_{ls} - 2\overset{*}{\zeta}_{lc} - \zeta_{ls}) + \text{M}\Omega^2\frac{N}{2}\zeta_{ls} - \text{M}\ddot{x}_h\frac{N}{2} \\
&\quad - 2\text{S}_\zeta\Omega^2\frac{N}{2}(\overset{*}{\zeta}_{lc} + \zeta_{ls}) - \text{M}\ddot{x}_h\frac{N}{2} \\
&= -\text{S}_\zeta\Omega^2\frac{N}{2}\overset{**}{\zeta}_{ls} - N\text{M}_b\ddot{x}_h \\
&= -\frac{N}{2}\text{S}_\zeta\ddot{\zeta}_{ls} - N\text{M}_b\ddot{x}_h
\end{aligned}$$

Y = Total Edge Force

$$\begin{aligned}
Y &= \sum_{m=1}^{N}(-\text{S}_x\cos\psi_m + \text{S}_r\sin\psi_m) \\
&= \sum_{m=1}^{N} -\cos\psi_m[\text{S}_\zeta\ddot{\zeta}^{(m)} + \text{M}\Omega^2\zeta^{(m)} - \text{M}(\ddot{x}_h\sin\psi_m - \ddot{y}_h\cos\psi_m)] \\
&\quad + \sum_{m=1}^{N} \sin\psi_m[-2\text{S}_\zeta\Omega\dot{\zeta}^{(m)} - \text{M}(\ddot{x}_h\cos\psi_m - \ddot{y}_h\sin\psi_m)] \\
&= \text{S}_\zeta\Omega^2\frac{N}{2}(\overset{**}{\zeta}_{lc} + 2\overset{*}{\zeta}_{ls} - \zeta_{lc}) - \text{M}\Omega^2\frac{N}{2}\zeta_{lc} - \text{M}\ddot{y}_h\frac{N}{2} \\
&\quad - 2\text{S}_\zeta\Omega^2\frac{N}{2}(\overset{*}{\zeta}_{ls} - \zeta_{lc}) - \text{M}\ddot{y}_h\frac{N}{2} \\
&= \text{S}_\zeta\Omega^2\frac{N}{2}\overset{**}{\zeta}_{lc} - \text{M}_b N\ddot{y}_h
\end{aligned}$$

where N is the number of blades and M_b is the total blade mass. The C_x and C_y are the damping coefficients of the supporting structure.

The body equations can be rewritten as

$$\ddot{x}_h(\text{M}_x + N\text{M}_b) + \text{C}_x\dot{x}_h + k_x x_h + \frac{N}{2}\text{S}_\zeta\ddot{\zeta}_{ls} = 0$$

$$\ddot{y}_h(\text{M}_y + N\text{M}_b) + \text{C}_y\dot{y}_h + k_y y_h - \frac{N}{2}\text{S}_\zeta\ddot{\zeta}_{lc} = 0$$

Imagine that there are no coupling terms, then one can calculate natural frequencies of support as

$$\omega_x^2 = \frac{k_x}{\text{M}_x + N\text{M}_b}$$

$$\omega_y^2 = \frac{k_y}{\mathrm{M}_y + N\mathrm{M}_b}$$

Also, defining

$$\mathrm{C}_x^* = \frac{\mathrm{C}_x}{\Omega(\mathrm{M}_x + N\mathrm{M}_b)}$$

$$\mathrm{C}_y^* = \frac{\mathrm{C}_y}{\Omega(\mathrm{M}_y + N\mathrm{M}_b)}$$

The equations of motion expressed in nondimensional form

$$\begin{bmatrix} 1.0 & 0 & 0 & -\mathrm{S}_\zeta^* \\ 0 & 1.0 & \mathrm{S}_\zeta^* & 0 \\ 0 & \frac{1}{2}\frac{\mathrm{S}_\zeta^*}{\mathrm{M}_x^*} & 1 & 0 \\ \frac{1}{2}\frac{\mathrm{S}_\zeta^*}{\mathrm{M}_y^*} & 0 & 0 & 1 \end{bmatrix} \begin{bmatrix} \overset{**}{\zeta}_{lc} \\ \overset{**}{\zeta}_{ls} \\ \overset{**}{x}_h \\ \overset{**}{y}_h \end{bmatrix} + \begin{bmatrix} \mathrm{C}_\zeta^* & 2 & 0 & 0 \\ -2 & \mathrm{C}_\zeta^* & 0 & 0 \\ 0 & 0 & \mathrm{C}_x^* & 0 \\ 0 & 0 & 0 & \mathrm{C}_y^* \end{bmatrix} \begin{bmatrix} \overset{*}{\zeta}_{lc} \\ \overset{*}{\zeta}_{ls} \\ \overset{*}{x}_h \\ \overset{*}{y}_h \end{bmatrix}$$

$$+ \begin{bmatrix} \nu_\zeta^2 - 1 & \mathrm{C}_\zeta^* & 0 & 0 \\ -\mathrm{C}_\zeta^* & \nu_\zeta^2 - 1 & 0 & 0 \\ 0 & 0 & \frac{\omega_x^2}{\Omega^2} & 0 \\ 0 & 0 & 0 & \frac{\omega_y^2}{\Omega^2} \end{bmatrix} \begin{bmatrix} \zeta_{lc} \\ \zeta_{ls} \\ x_h \\ y_h \end{bmatrix} = 0$$

where

$$\begin{aligned} \mathrm{S}_\zeta^* &= \frac{{}_R\mathrm{S}_\zeta}{\mathrm{I}_\zeta} \cong \frac{{}_R\mathrm{S}_\zeta}{\mathrm{I}_b} \\ &= \tfrac{3}{2} \text{for uniform blades} \\ &\quad \mathrm{I}_b \text{ is blade inertia } = \mathrm{M}_b\tfrac{R^2}{3} \text{ for uniform blade} \\ \mathrm{M}_x^* &= \frac{(\mathrm{M}_x + N\mathrm{M}_b)R^2}{N\mathrm{I}_b} \\ &= 3\left(\frac{\mathrm{M}_x}{N\mathrm{M}_b} + 1\right) \text{for uniform blades} \\ \mathrm{M}_y^* &= \frac{(\mathrm{M}_y + N\mathrm{M}_b)R^2}{N\mathrm{I}_b} \\ &= 3\left(\frac{\mathrm{M}_y}{N\mathrm{M}_b} + 1\right) \text{for uniform blades} \\ N\mathrm{M}_b &= \text{Total rotor mass} \end{aligned}$$

For uniform blades

$$\frac{\mathrm{S}_\zeta^*}{\mathrm{M}_x^*} = \frac{1}{2(\frac{\mathrm{M}_y}{N\mathrm{M}_b} + 1)} \cong \frac{1}{2}\frac{\text{Rotor mass}}{\text{Support mass}} \quad (\text{Support mass} = \mathrm{M}_y + N\mathrm{M}_b)$$

$$\frac{\mathrm{S}_\zeta^*}{\mathrm{M}_y^*} = \frac{1}{2(\frac{\mathrm{M}_x}{N\mathrm{M}_b} + 1)} \cong \frac{1}{2}\frac{\text{Rotor mass}}{\text{Support mass}}$$

The support mass is much larger than the rotor mass. In the above equations, the hub displacement x_h and y_h are also nondimensional with respect to rotor radius R.

$$\begin{aligned} \overline{x}_h &= \tfrac{x_h}{R} \\ \overline{y}_h &= \tfrac{y_h}{R} \end{aligned}$$

The governing equations are four second order differential equations. These can be solved either through determinate expansion or through the eigen analysis. Let us examine the first approach of determinate expansion. The stability determinant is

$$\begin{vmatrix} (s^2 + \mathrm{C}_\zeta^* s + \nu_\zeta^2 - 1) & (2s + \mathrm{C}_\zeta^*) & 0 & -s_\zeta^* s^2 \\ -(2s + \mathrm{C}_\zeta^*) & (s^2 + \mathrm{C}_\zeta^* s + \nu_\zeta^2 - 1) & s_\zeta^* s^2 & 0 \\ 0 & (\frac{1}{2}\frac{s_\zeta^*}{\mathrm{M}_\zeta^*}) s^2 & (s^2 + \mathrm{C}_x^* s + \frac{\omega_x^2}{\Omega^2}) & 0 \\ -(\frac{1}{2}\frac{s_\zeta^*}{\mathrm{M}_\zeta^*}) s^2 & 0 & 0 & (s^2 + \mathrm{C}_\zeta^* s + \nu_\zeta^2 - 1) \end{vmatrix} = 0$$

This is an eighth order polynomial. The solution gives eight eigenvalues, which means four complex conjugate pairs. From the physics, the divergence instability is not possible. The ground resonance is a dynamic instability where one of the modes becomes unstable, i. e. , zero damping condition.

For divergence stability

$$[(\nu_\zeta^2 - 1)^2 + \mathrm{C}_\zeta^{*2}](\frac{\omega_x}{\Omega})^2(\frac{\omega_y}{\Omega})^2 > 0$$

This is always satisfied. Let us first consider the uncoupled dynamics, obtained by setting S_ζ^* equal to zero. The blade lag motion is damped and its eigenvalue in the rotating frame is

$$s_R = -\frac{\mathrm{C}_\zeta^*}{2} \pm i\sqrt{\nu_\zeta^2 - \left(\frac{\mathrm{C}_\zeta^*}{2}\right)^2}$$

and in the fixed frame, the eigenvalue is

$$s = s_R \pm i \quad (\mathrm{n} = 1)$$

This consists of two types of modes

(a) High frequency mode $\qquad s = s_R + i$

Frequency $= \mathrm{I}_m s_R + 1$ per rev.

Frequency of oscillation is always greater than the rotational speed, and corresponds to a progressive whirling motion of the rotor cg.

(b) Low frequency mode $\qquad s = s_R - i$

Frequency $= \mathrm{I}_m s_R - 1$ per rev.

There are two possibilities. For stiff lag rotors ($\mathrm{I}_m s_R > 1$), it results into a regressive whirling motion of the rotor cg at a frequency of ($\mathrm{I}_m s_R - 1$) per rev. For soft lag rotors ($\mathrm{I}_m s_R < 1$), it results into a progressive whirling mode of the rotor cg at a frequency of ($1 - \mathrm{I}_m s_R$) per rev. The last possibility is a typical example of an articulated rotor.

Let us examine the uncoupled inplane support eigenvalues in x and y directions.

$$s = -\frac{\mathrm{C}_x^*}{2} \pm i\sqrt{\left(\frac{\omega_x}{\Omega}\right)^2 - \left(\frac{\mathrm{C}_x^*}{2}\right)^2}$$

$$s = -\frac{\mathrm{C}_y^*}{2} \pm i\sqrt{\left(\frac{\omega_y}{\Omega}\right)^2 - \left(\frac{\mathrm{C}_y^*}{2}\right)^2}$$

These are two complex conjugate pairs in the fixed reference frame. In total, these are four conjugate pairs. Looking at the real parts, one finds that the uncoupled rotor and support motion is stable. Therefore, the ground resonance instability is a possibility due to inertial coupling s_ζ^*.

For a configuration with zero damping and zero inertial coupling, there are four frequencies, high frequency lag $\nu_\zeta + 1$, low frequency lag $1 - \nu_\zeta$, longitudinal support frequency ω_x and lateral support frequency ω_y. With the inclusion of coupling terms, the different modes coalesce resulting in instability. This is a dynamic instability and is of catastrophic type.

In the first figure the Coleman diagram is plotted for an articulated rotor with soft inplane frequency. The Coleman diagram consists of a plot of dimensional frequencies as a function of rotational speed. The frequencies corresponding to different modes in the fixed frame are obtained either from the eigen-solutions or from the roots of the eighth order polynomial. The following data is used for calculations.

$$\begin{array}{ll} \mathrm{S}^*_\zeta = 1.5 & \mathrm{C}^*_\zeta = \mathrm{C}^*_x = \mathrm{C}^*_y = 0 \\ \mathrm{M}^*_x = 68.175 & \mathrm{M}^*_y = 29.708 \\ \nu_\zeta = .285/\text{rev} & \omega_x = 12.148 \text{ rad/sec},\ \omega_y = 18.402 \text{ rad/sec} \end{array}$$

There are two instability bands, caused by coalescence of rotor and body modes. For a stable condition, there are four distinct eigenvalues. For an unstable condition, two frequencies merge resulting in three distinct eigenvalues. Also the real part of the eigenvalue which represents damping of the mode becomes positive. In the next figure, the damping ratio of the unstable mode is presented. The value of damping ratio of 0.1 is quite large and represents violent instability. This also shows that a large lag damping is required to stabilize this instability.

In the next figure, the Coleman diagram is plotted for an articulated rotor with stiff inplane frequency. The following data are used for calculations.

$$\begin{array}{ll} \mathrm{S}^*_\zeta = 3.19 & \mathrm{C}^*_\zeta = \mathrm{C}^*_x = \mathrm{C}^*_y = 0 \\ \mathrm{M}^*_x = 178.77 & \mathrm{M}^*_y = 77.902 \\ \nu_\zeta = 1.3/\text{rev} & \omega_x = 12.148 \text{ rad/sec},\ \omega_y = 18.402 \text{ rad/sec} \end{array}$$

There is no instability condition for stiff inplane rotors.

For a case of no-damping

$$\mathrm{C}^*_\zeta = \mathrm{C}^*_x = \mathrm{C}^*_y = 0$$

The stability determinant becomes

$$\begin{vmatrix} s^2 + \nu_\zeta^2 - 1 & 2s & 0 & -s^*_\zeta s^2 \\ -2s & s^2 + \nu_\zeta^2 - 1 & s^*_\zeta s^2 & 0 \\ 0 & \frac{1}{2}\left(\frac{s^*_\zeta}{\mathrm{M}^*_x}\right) s^2 & s^2 + \frac{\omega_x^2}{\Omega^2} & 0 \\ -\frac{1}{2}\left(\frac{s^*_\zeta}{\mathrm{M}^*_y}\right) s^2 & 0 & 0 & s^2 + \frac{\omega_y^2}{\Omega^2} \end{vmatrix} = 0$$

This gives

$$\begin{aligned} &[(s^2 + \nu_\zeta^2 - 1)^2 + 4s^2](s^2 + \tfrac{\omega_x^2}{\Omega^2})(s^2 + \tfrac{\omega_y^2}{\Omega^2}) - (s^2 + \nu_\zeta^2 - 1)\frac{s^{*\,2}_\zeta}{\mathrm{M}^*_x \mathrm{M}^*_y} \\ &\quad \times s^4[\mathrm{M}^*_y(s^2 + \omega_y^2) + \mathrm{M}^*_x(s^2 + \omega_x^2)] + \frac{s^{*\,4}_\zeta}{\mathrm{M}^*_x \mathrm{M}^*_y} s^8 = 0 \end{aligned}$$

The critical condition of zero system damping can be calculated by substituting $s = i\omega$ in the above equation. The numerical solution of the polynomial represents the boundary line between stable and unstable conditions.

Deutsch Stability Criteria

Using an approximate stability criteria, a simple expression for damping required to stabilize ground resonance is obtained.

Longitudinal mode:

$$\text{Assumed } \frac{\omega}{\Omega} \cong \frac{\omega_x}{\Omega} = 1 - \nu_\zeta \text{ and } \omega_x \neq \omega_y \text{ For stability}$$

$$\mathrm{C}^*_\zeta \mathrm{C}^*_x > \frac{(1-\nu_\zeta)}{4\nu_\zeta} \left(\frac{\omega_x}{\Omega}\right)^2 \frac{{s^*_\zeta}^2}{\mathrm{M}^*_x}$$

Lateral mode:

$$\text{Assumed } \frac{\omega}{\Omega} \cong \frac{\omega_y}{\Omega} = 1 - \nu_\zeta \text{ and } \omega_x \neq \omega_y \text{ For stability}$$

$$\mathrm{C}^*_\zeta \mathrm{C}^*_y > \frac{(1-\nu_\zeta)}{4\nu_\zeta} \left(\frac{\omega_y}{\Omega}\right)^2 \frac{{s^*_\zeta}^2}{\mathrm{M}^*_y}$$

For a stiff-lag rotor, ($\nu_\zeta > 1$), the right hand side is negative and the system is always stable. For a soft-lag rotor, ($\nu_\zeta < 1$), the product of lag damping and support damping must be greater than the critical values given above for longitudinal and lateral modes. A larger lag damping is required for

(a) small lag frequency (typical of articulated rotors)

(b) large support frequency (ω_x or ω_y)

(c) large inertial coupling ${s^*_\zeta}^2/\mathrm{M}^*_x$ or ${s^*_\zeta}^2/\mathrm{M}^*_y$ ($\cong \frac{3}{4}\frac{\text{rotor mass}}{\text{support mass}}$)

For an isotropic support condition ($\omega_x = \omega_y$). For stability

$$\mathrm{C}^*_\zeta \mathrm{C}^*_y > \frac{(1-\nu_\zeta)}{2\nu_\zeta} \left(\frac{\omega_y}{\Omega}\right)^2 \frac{{s^*_\zeta}^2}{\mathrm{M}^*_y}$$

One requires twice the damping needed for an anisotropic case ($\omega_x \neq \omega_y$). This is because the longitudinal and lateral support frequencies become equal resulting in the whirling motion of the hub which couples well with the whirling motion of the low-frequency lag mode.

Ex. The shake test was performed on the helicopter on its landing gear and the natural frequencies were obtained as 1.2 and 1.8 Hz respectively in longitudinal and lateral directions. The damping ratios were calculated as 2% of critical value for both the modes. The helicopter rotor was four-bladed, articulated with 6% hinge offset. The blades are uniform and form about 10% of the total weight. You would like to check whether the rotor is stable from ground resonance at an operating speed of 360 RPM. Write the stability equation in the form of determinant.

$$\omega = 6\text{Hz}$$
$$\omega_x = \frac{1.2}{6} = .2/\text{rev}$$
$$\omega_y = \frac{1.8}{6} = .3/\text{rev}$$
$$\zeta_x = \zeta_x = .02$$

$$C_x^* = 2\zeta_x\omega_x = .008$$
$$C_y^* = 2\zeta_y\omega_y = .012$$
$$\nu_\zeta^2 = .09 \qquad \nu_\zeta = .3$$
$$I_\zeta^* = 1$$
$$s_\zeta = \tfrac{mR^2}{2} \qquad I_b = \tfrac{mR^3}{3} \qquad s_\zeta^* = \tfrac{3}{2}$$

$$M_x^* = \frac{R^2(M_x + NM_b)}{NI_b} = \frac{M_x + NM_b}{NM_b\frac{1}{3}} = 30 = M_y^*$$

Stability determinant

$$\begin{vmatrix} s^2+.09-1 & 2s & 0 & -\frac{3}{2}s^2 \\ -2s & s^2+.09-1 & \frac{3}{2}s^2 & 0 \\ 0 & \frac{3}{2}s^2 & 60(s^2+.008s+.04) & 0 \\ -\frac{3}{2}s^2 & 0 & 0 & 60(s^2+.012s+.09) \end{vmatrix} = 0$$

Expansion of the determinant will give 8th order polynomial. Solution will be 4 complex conjugate pairs. Nature of the roots tells us whether the system is stable or not.

6.2 Ground Resonance of Two-Bladed Rotors

Let us consider the ground resonance stability of a two-bladed rotor. Again, assume the rotor is fully tracked and the blade undergoes lag degree of motion.

Rotating frame:

$\zeta^{(1)} =$ lag motion of blade 1

$\zeta^{(2)} =$ lag motion of blade 2

Fixed frame:

$$\begin{aligned} \zeta_o &= \text{collective lag motion} \\ &= \tfrac{1}{2}\left(\zeta^{(2)} + \zeta^{(1)}\right) \\ \zeta_1 &= \text{differential collective lag motion} \\ &= \tfrac{1}{2}\left(\zeta^{(2)} - \zeta^{(1)}\right) \end{aligned}$$

Also,

$$\zeta^{(1)} = \zeta_o - \zeta_1$$
$$\zeta^{(2)} = \zeta_o + \zeta_1$$

Let us examine the influence of lag motion on rotor cg.

$\underline{\zeta_o \text{ motion}}$ cg stays at center

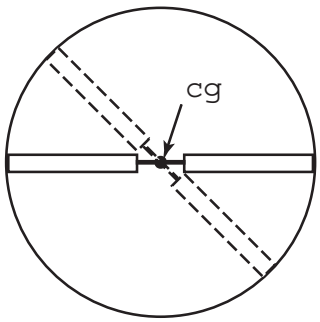

$\underline{\zeta_1 \text{ motion}}$ Assuming

$$\zeta^{(1)} = \zeta_o - \zeta_{lc}\cos\psi - \zeta_{ls}\sin\psi$$

$$\zeta^{(2)} = \zeta_o + \zeta_{lc}\cos\psi + \zeta_{ls}\sin\psi$$

This gives

$$\zeta_1 = \zeta_{lc}\cos\psi + \zeta_{ls}\sin\psi$$

Two cases.

(a) $\zeta_1 = \zeta_{lc}\cos\psi$

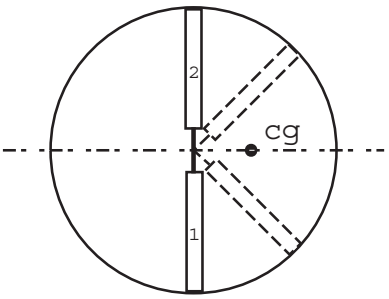

A lateral shift of rotor cg in positive x-direction.

(b) $\zeta_1 = \zeta_{ls}\sin\psi$

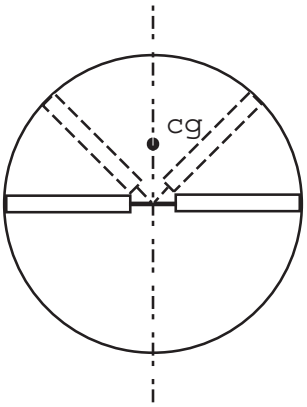

A longitudinal shift of cg in negative x-direction.

Therefore, the differential collective lag motion ζ_1 coupled with support motion to cause ground resonance instability for the 2-bladed rotor.

The uncoupled lag equations for blades in the rotating frame are

$$\overset{**(1)}{\zeta} + C_\zeta^* \overset{*(1)}{\zeta} + \nu_\zeta^2 \zeta^{(1)} = 0$$

$$\overset{**(2)}{\zeta} + C_\zeta^* \overset{*(2)}{\zeta} + \nu_\zeta^2 \zeta^{(2)} = 0$$

Transformed rotor equations in fixed frame are

$$\overset{**}{\zeta}_o + C_\zeta^* \overset{*}{\zeta}_o + \nu_\zeta^2 \zeta_o = 0$$

$$\overset{**}{\zeta}_1 + C_\zeta^* \overset{*}{\zeta}_1 + \nu_\zeta^2 \zeta_1 = 0$$

Now, if there is a hub motion of x_h and y_h superimposed on lag motion, the lag equations become

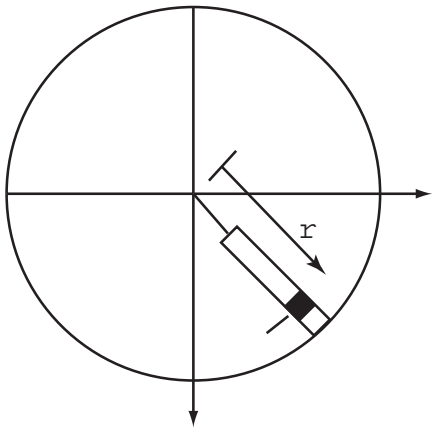

$$\mathrm{I}_\zeta(\overset{**(2)}{\zeta} + \mathrm{C}^*_\zeta \overset{*(2)}{\zeta} + \nu^2_\zeta \zeta^{(2)}) + \mathrm{S}_\zeta(\overset{**}{x}_h \sin\psi - \overset{**}{y}_h \cos\psi) = 0$$

$$\mathrm{I}_\zeta(\overset{**(1)}{\zeta} + \mathrm{C}^*_\zeta \overset{*(1)}{\zeta} + \nu^2_\zeta \zeta^{(1)}) - \mathrm{S}_\zeta(\overset{**}{x}_h \sin\psi - \overset{**}{y}_h \cos\psi) = 0$$

and the rotor equations become

$$\overset{**}{\zeta}_o + \mathrm{C}^*_\zeta \overset{*}{\zeta}_o + \nu^2_\zeta \zeta_o = 0$$

$$\mathrm{I}_\zeta(\overset{**}{\zeta}_1 + \mathrm{C}^*_\zeta \overset{*}{\zeta}_1 + \nu^2_\zeta \zeta_1) + \mathrm{S}_\zeta(\overset{**}{x}_h \sin\psi - \overset{**}{y}_h \cos\psi) = 0$$

The first collective lag equation is unaffected by hub motion. The differential collective equation however gets modified with the hub motion. Again, assuming vehicle is supported by two sets of springs and dampers represented by k_x, C_x, k_y, C_y. The body equations of motion are

$$\mathrm{M}_x \ddot{x}_h + \mathrm{C}\dot{x}_h + k_x x_h = H$$

$$\mathrm{M}_y \ddot{y}_h + \mathrm{C}\dot{y}_h + k_y y_h = Y$$

The inplane hub forces H and Y are obtained from blade shear forces

$$\mathrm{S}_r = -2\Omega\dot{\zeta}\mathrm{S}_\zeta - \mathrm{M}_b(\ddot{x}_h \cos\psi + \ddot{y}_h \sin\psi)$$

$$\mathrm{S}_x = \mathrm{S}_\zeta(\Omega^2\zeta - \ddot{\zeta}) - \mathrm{M}_b(\ddot{x}_h \sin\psi - \ddot{y}_h \cos\psi)$$

and

$$\begin{aligned} H &= \sum_{m=1}^{2} (\mathrm{S}_x^{(m)} \sin\psi_m + \mathrm{S}_r^{(m)} \cos\psi_m) \\ &= -2\mathrm{M}_b \ddot{x}_h + 2\mathrm{S}_\zeta[(\Omega^2\zeta_1 - \ddot{\zeta}_1)\sin\psi - 2\Omega\dot{\zeta}_1 \cos\psi] \\ Y &= \sum_{m=1}^{2} (-\mathrm{S}_x^{(m)} \cos\psi_m + \mathrm{S}_r^{(m)} \sin\psi_m) \\ &= -2\mathrm{M}_b \ddot{y}_h + 2\mathrm{S}_\zeta[(\ddot{\zeta}_1 - \Omega^2\zeta_1)\cos\psi - 2\Omega\dot{\zeta}_1 \sin\psi] \end{aligned}$$

Again using the previous definitions, the coupled rotor-body equations for a two-bladed rotor can be written as

$$\begin{bmatrix} 1.0 & \mathrm{S}^*_\zeta \sin\psi & -\mathrm{S}^*_\zeta \cos\psi \\ \frac{\mathrm{S}^*_\zeta}{\mathrm{M}^*_\zeta}\sin\psi & 1.0 & 0 \\ -\frac{\mathrm{S}^*_\zeta}{\mathrm{M}^*_\zeta}\cos\psi & 0 & 1.0 \end{bmatrix} \begin{bmatrix} \overset{**}{\zeta}_1 \\ \overset{**}{x}_h \\ \overset{**}{y}_h \end{bmatrix} + \begin{bmatrix} \mathrm{C}^*_\zeta & 0 & 0 \\ 2\frac{\mathrm{S}^*_\zeta}{\mathrm{M}^*_x}\cos\psi & \mathrm{C}^*_x & 0 \\ 2\frac{\mathrm{S}^*_\zeta}{\mathrm{M}^*_y}\sin\psi & 0 & \mathrm{C}^*_y \end{bmatrix} \begin{bmatrix} \overset{*}{\zeta}_1 \\ \overset{*}{x}_h \\ \overset{*}{y}_h \end{bmatrix}$$

$$+ \begin{bmatrix} \nu^2_\zeta & 0 & 0 \\ -\frac{\mathrm{S}^*_\zeta}{\mathrm{M}^*_x}\sin\psi & \frac{\omega^2_x}{\Omega^2} & 0 \\ \frac{\mathrm{S}^*_\zeta}{\mathrm{M}^*_y}\cos\psi & 0 & \frac{\omega^2_y}{\Omega^2} \end{bmatrix} \begin{bmatrix} \zeta_1 \\ x_h \\ y_h \end{bmatrix} = 0$$

These are three second order differential equations and can be solved either through determinant expansion or through the eigen-analysis.

6.3 Air Resonance

An air resonance is similar to ground resonance but occurs on an airborne vehicle. It is caused by coupling of low frequency blade flap and lag modes and rigid body airframe modes. Aerodynamic forces are needed to determine this instability. Air resonance is primarily a problem for soft-inplane hingeless and bearingless rotors.

In general, hingeless and bearingless aeromechanical stability is more difficult to predict compared to articulated rotors. The frequencies of rotor flap coupled with body angular motions coalesce with the rotor lag frequency. Due to the presence of the flap motion, aerodynamic forces become important. For hingeless and bearingless rotors, flap, lag, and torsion can be highly coupled, and the torsion motion can affect ground and air resonance. The damping and frequency characteristics of coupled hingeless rotor-body modes often make the associated instabilities a mild phenomena.

Compared to ground resonance, where the body modes are relatively clear, in air resonance they are more complex. In ground resonance the body modes are determined by the rotor-body mass reacting against the fixed ground. In air resonance there is offcourse no fixed ground against which the rotor-body mass can react. Here, the body modes are the fundamental free-free modes of the rotor-body reacting against each other through the interposed blade flap spring (mechanical or virtual) stiffness. Hence the body modes are determined by the flap spring stiffness, rotor inertia, body inertia, and rotor aerodynamics. The modes and frequencies are not well defined and show great variety from one rotor to another. The coalescences are also more obscure.

The basic mechanism of air resonance involves flap, lag, body pitch and body roll motions. For a simple analysis, blades are assumed rigid and undergo flap and lag motions about hinges. The body is also assumed rigid and undergoes pitch and roll motion about the body center of gravity. Body translation degrees of freedom are not included since they do not significantly influence air resonance stability. Let us study the behavior of the isolated modes in a step-wise manner.

The body pitch and roll degrees of freedom are shown in Fig. 6.1. If I_Y is the fuselage (or body) mass moment of inertia about the pitch axis, M_F is the fuselage mass, then the square of the body mass radius of gyration about the pitch axis, nondimensionalized with the square of the rotor radius, is given by

$$K^2_y = \frac{M_F}{I_y R^2}$$

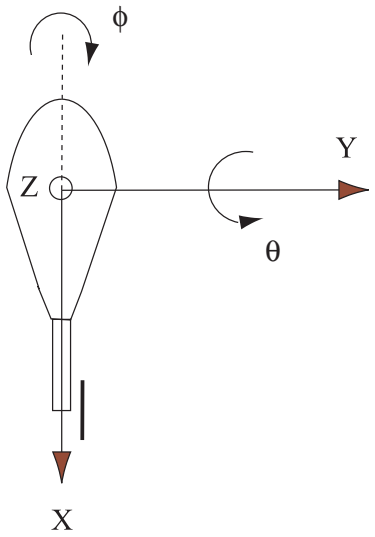

Figure 6.1: **Body pitch and roll degrees of freedom**

Similarly the square of the body mass radius of gyration about the roll axis, nondimensionalized with the square of the rotor radius, is given by

$$K_x^2 = \frac{M_F}{I_x R^2}$$

Typical values are

$$K_y^2 = \frac{\text{square of body mass radius of gyration}}{R^2} \approx 0.1 \text{ to } 0.4$$

$$K_x^2 \approx 0.025$$

The body pitch and roll frequencies, nondimensionalized with respect to the operating rotational speed Ω_0 typically varies between

$$\text{body pitch frequency} = \bar{\omega_\theta} = 0 \text{ to } 0.8/\text{rev}$$

$$\text{body roll frequency} = \bar{\omega_\phi} = 0 \text{ to } 0.4/\text{rev}$$

The mass ratio and distance of rotor hub above the rotor-body c.g. are typically

$$\frac{\text{rotor mass}}{\text{total mass}} = 0.1$$

$$\frac{h}{R} = 0.2$$

The characteristic plots shown in the subsequent sections correspond to the following values, where applicable.

$$\nu_\zeta = 0.7/\text{rev}$$

$$\nu_\beta = 1.1/\text{rev}$$

$$\gamma = 5 - -15$$

$$\sigma = 0.05$$

$$c_{l\alpha} = 5.73$$

$$c_{d0} = 0.01$$

The lag and flap frequencies above are typical values for soft inplane hingeless rotors.

6.3.1 Body Pitch and Roll with a Rigid Spinning Rotor

Consider a two degree of freedom system, as shown in Fig. 6.1, with body pitch and roll modes. Consider a spinning rotor attached at the top. When the rotor is rigid, i.e. has no flapping, the frequencies in vacuum represent those of a 2 degree of freedom gyroscope. The four eigenvalues of the system are

$$\eta = 0, 0, \pm j \frac{\Omega J}{\sqrt{I_\theta I_\phi}}$$

The zeroes represent the unconstrained rigid body pitch and roll motions. The imaginary pairs are the well known nutation frequency of a gyroscope. I_θ and I_ϕ are the rotor-body pitch and roll inertia about the rotor-body center of mass.

$$I_\theta = I_y + \frac{1}{2} N_b I_b + 3 N_b I_b h^2$$

$$I_\phi = I_x + \frac{1}{2} N_b I_b + 3 N_b I_b h^2$$

$J =$ rotor polar mass moment of inertia $= N_b I_b$

If the body vanishes, we have

$$I_\theta = I_\phi = \frac{1}{2} N_b I_b$$

and

$$\eta = 0, 0, \pm j 2\Omega$$

A well known result, where the gyroscopic nutation frequency is twice the rotational speed. The above results were in vacuum. In air, the spinning rigid rotor acts as a damper and the four eigenvalues of the system become

$$\eta = 0, 0, \sigma \pm j\omega$$

where

$$\begin{aligned} \sigma &= -\left(\frac{I_\theta + I_\phi}{I_\theta I_\phi}\right) \frac{J\gamma}{32} \Omega \\ \omega &= \frac{\Omega J}{\sqrt{I_\theta I_\phi}} \sqrt{1 + \left(\frac{\gamma}{16}\right)^2 \left[\frac{1}{2} - \frac{1}{4}\left(\frac{I_\theta}{I_\phi} + \frac{I_\phi}{I_\theta}\right)\right]} \end{aligned} \tag{6.1}$$

I_θ is greater than I_ϕ, hence the term associated with $(\gamma/16)^2$ in the expression for frequency is negative. For very high values of γ, the frequency can become imaginary and produce two real eigenvalues.

6.3.2 Rotor Flap and Lag

Consider the flapping motion in the rotating frame. Assuming an offset e/R and non-rotating frequency of $\omega_{\beta 0}$ rad/s, and rotational speed Ω, the rotating flap frequency ν_β is given by

$$\nu_\beta^2 = 1 + \frac{3}{2}\frac{e}{R} + \frac{\omega_{\beta 0}^2}{\Omega^2}$$

Another useful way of writing the frequency expression is to first denote the flap frequency at the operating RPM as p. That is

$$p^2 = 1 + \frac{3}{2}\frac{e}{R} + \frac{\omega_{\beta 0}^2}{\Omega_0^2}$$

Then

$$\omega_{\beta 0}^2 = \left(p^2 - 1 - \frac{3}{2}\frac{e}{R}\right)\Omega_0^2$$

The rotating flap frequency expression can now be written as

$$\nu_\beta^2 = 1 + \left(p^2 - 1 - \frac{3}{2}\frac{e}{R}\right)\frac{\Omega_0^2}{\Omega^2}$$

where the flap frequency at the operating RPM, p, occurs explicitly. We shall drop the term $3e/2R$ at this point, as it adds no new physics, inclusion of this term by interested readers will be straight-forward. Thus we have

$$\nu_\beta^2 = 1 + \left(p^2 - 1\right)\frac{\Omega_0^2}{\Omega^2}$$

Recall that the flap perturbation equation in hover was

$$\overset{**}{\beta} + \frac{\gamma}{8}\overset{*}{\beta} + \nu_\beta^2\beta = 0$$

with characteristic stability roots

$$-\frac{\gamma}{16} \pm i\sqrt{\nu_\beta^2 - \left(\frac{\gamma}{16}\right)^2} \text{ in /rev}$$

In dimensional form was

$$\ddot{\beta} + \frac{\gamma}{8}\Omega\dot{\beta} + \nu_\beta^2\Omega^2\beta = 0$$

with characteristic stability roots

$$\sigma \pm i\omega = -\frac{\gamma}{16}\Omega \pm i\Omega\sqrt{\nu_\beta^2 - \left(\frac{\gamma}{16}\right)^2} \text{ in rad/s}$$

Using the expression for flap frequency given above we can write

$$\begin{aligned}\sigma =& -\frac{\gamma}{16}\Omega \\ \omega =& \Omega\left[1 + \left(p^2 - 1\right)\frac{\Omega_0^2}{\Omega^2} - \left(\frac{\gamma}{16}\right)^2\right]^{1/2}\end{aligned} \tag{6.2}$$

Nondimensionalized with respect to the operating RPM, Ω_0, we have

$$\begin{aligned}\bar{\sigma} =& \frac{\sigma}{\Omega_0} = -\frac{\gamma}{16}\bar{\Omega} \\ \bar{\omega} =& \frac{\omega}{\Omega_0} = \bar{\Omega}\left[1 + \left(p^2 - 1\right)/\bar{\Omega}^2 - \left(\frac{\gamma}{16}\right)^2\right]^{1/2}\end{aligned} \tag{6.3}$$

The frequencies in the fixed frame are simply shifted by integer multiples of the rotational speed. Consider for the sake of discussion we have a three or a four bladed rotor. Then the frequencies of the fixed frame cyclic flapping modes, β_{1c} and β_{1s}, are given by

$$\omega_F = |\omega \pm \Omega| \quad \text{in rad/s} \quad \text{or,} \quad \text{in nondimensional form} \quad \bar{\omega}_F = |\bar{\omega} \pm \bar{\Omega}|$$

The high frequencies, obtained using the positive sign, is always positive. The low frequencies, obtained using the negative sign, decreases with increase in Ω, and in air (i.e. for a non-zero Lock number) eventually hits zero. With further increase in Ω it continues to become more and more negative, however, because the physical frequency of oscillation is the absolute value of this number, the absolute value is plotted, showing an increase with increase in Ω. Figure 6.2(a) plots the fixed frame frequencies in rad/s. Figure 6.2(b) is an identical plot, only this time in nondimensional form. Figure 6.2(a) uses the expression in eqn. 6.2. Note that for $\Omega = 0$

$$\omega_F = \Omega \pm \left[\Omega^2 + \left(p^2 - 1\right)\Omega_0^2 - \Omega^2 \left(\frac{\gamma}{16}\right)^2\right]^{1/2} = \left[\left(p^2 - 1\right)\Omega_0^2\right]^{1/2} = \omega_{\beta 0}$$

Figure 6.2(b) uses the expression in eqn. 6.3. Note that for $\bar{\Omega} = 0$

$$\bar{\omega}_F = \bar{\Omega} \pm \left[\bar{\Omega}^2 + p^2 - 1 - \bar{\Omega}^2 \left(\frac{\gamma}{16}\right)^2\right]^{1/2} = \left[\left(p^2 - 1\right)\right]^{1/2} = \frac{\omega_{\beta 0}}{\Omega_0}$$

The magnitudes of β_{1c} and β_{1s} define the angular motion of the rotor disc plane with respect to the body. Note that, $\beta_{1c} - \theta$ and $\beta_{1s} - \phi$ define the angular motion of the rotor disc plane with respect to a fixed-space reference frame, for the simple case when the motions are in phase. For example, if $\beta_{1c} = \theta$ implies that the spinning rotor remains fixed in space due to gyroscopic inertia as the body pitches beneath it.

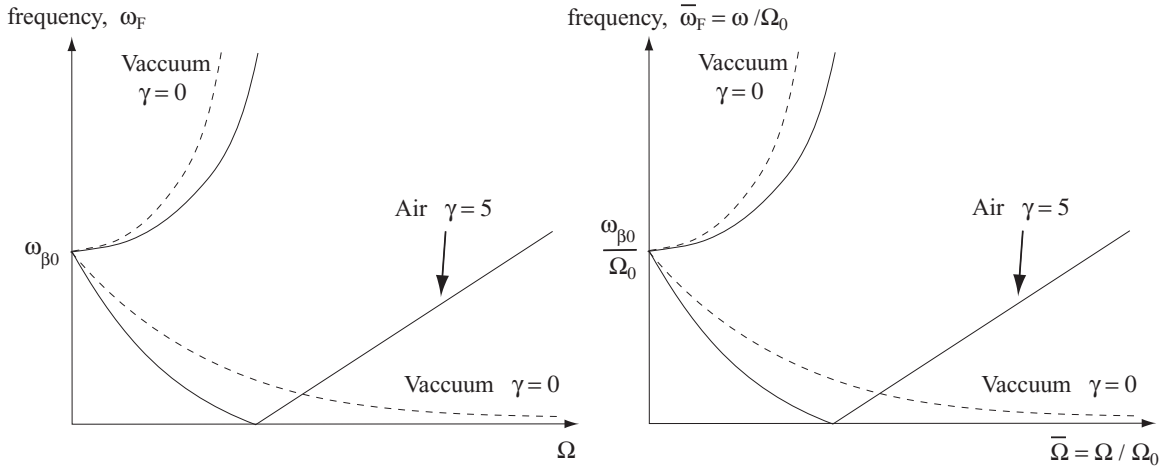

(a) Frequencies in radians /sec

(b) Frequencies nondimensionalized with respect to operating RPM Ω_0

Figure 6.2: **Rotor Flap Frequencies in the Fixed Frame**

Consider the lagging motion in the rotating frame. The rotating lag frequency ν_ζ is given by

$$\nu_\zeta^2 = \frac{3}{2}\frac{e}{R} + \frac{\omega_{\zeta 0}^2}{\Omega^2}$$

If the lag frequency at the operating RPM is q, then

$$q^2 = \frac{3}{2}\frac{e}{R} + \frac{\omega_{\zeta 0}^2}{\Omega_0^2}$$

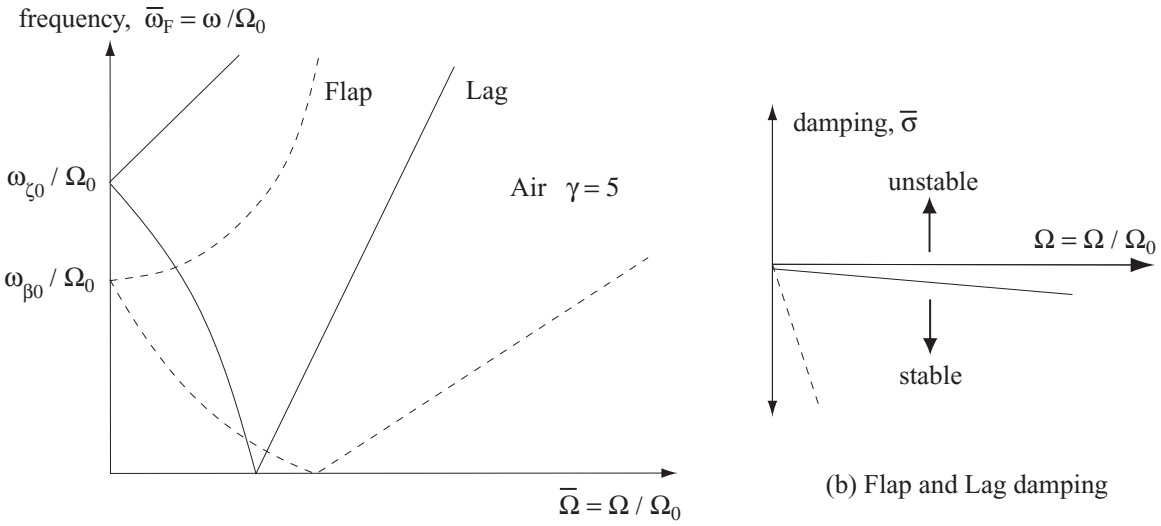

(a) Flap and Lag frequencies nondimensionalized with respect to operating RPM Ω_0

(b) Flap and Lag damping

Figure 6.3: **Rotor Flap and Lag Frequencies, and damping in the Fixed Frame**

It follows

$$\left(q^2 - \frac{3}{2}\frac{e}{R}\right)\Omega_0^2 = \omega_{\zeta 0}^2$$

$$\nu_\zeta^2 = \frac{3}{2}\frac{e}{R} + \left(q^2 - \frac{3}{2}\frac{e}{R}\right)\frac{\Omega_0^2}{\Omega^2}$$

where the lag frequency at the operating RPM, q, occurs explicitly. Dropping the term $3e/2R$, we have

$$\nu_\zeta^2 = q^2\,\frac{\Omega_0^2}{\Omega^2}$$

The frequencies in the fixed frame, of the 1st cyclic lag modes ζ_{1c} and ζ_{1s}, are then simply shifted by the rotational speed. In /rev they are

$$\begin{aligned} 1 + \nu_\zeta &= 1 + \left[\frac{3}{2}\frac{e}{R} + \frac{\omega_{\zeta 0}^2}{\Omega^2}\right]^{1/2} \quad \text{high frequency} \\ |1 - \nu_\zeta| &= \left|1 - \left[\frac{3}{2}\frac{e}{R} + \frac{\omega_{\zeta 0}^2}{\Omega^2}\right]^{1/2}\right| \quad \text{low frequency} \end{aligned} \tag{6.4}$$

In rad/s they are

$$\begin{aligned} \Omega + \omega_\zeta &= \Omega + \left[\frac{3}{2}\frac{e}{R}\Omega^2 + \omega_{\zeta 0}^2\right]^{1/2} \quad \text{high frequency} \\ |\Omega - \omega_\zeta| &= \left|\Omega + \left[\frac{3}{2}\frac{e}{R}\Omega^2 + \omega_{\zeta 0}^2\right]^{1/2}\right| \quad \text{low frequency} \end{aligned} \tag{6.5}$$

which shows the variation with RPM Ω. A convenient form is to nondimensionalize with the operating RPM Ω_0. Divide the above expressions by Ω_0 to obtain

$$\begin{aligned} \bar{\Omega} + \bar{\omega_\zeta} =& \bar{\Omega} + \bar{\Omega} \left[\frac{3}{2}\frac{e}{R} + \frac{\omega_{\zeta 0}^2/\Omega_0^2}{\bar{\Omega}^2} \right]^{1/2} \quad \text{high frequency} \\ |\bar{\Omega} - \bar{\omega_\zeta}| =& \left| \bar{\Omega} - \bar{\Omega} \left[\frac{3}{2}\frac{e}{R} + \frac{\omega_{\zeta 0}^2/\Omega_0^2}{\bar{\Omega}^2} \right]^{1/2} \right| \quad \text{low frequency} \end{aligned} \tag{6.6}$$

For $\Omega = 0$ (or $\bar{\Omega} = 0$), the high and low frequencies are the same and equal $\omega_{\zeta 0}$ (or $\omega_{\zeta 0}/\Omega_0$). To have the operating lag frequency q explicitly, use

$$\omega_{\zeta 0}^2 = \left(q^2 - \frac{3}{2}\frac{e}{R} \right) \Omega_0^2$$

to obtain the fixed frame frequencies as

$$\begin{aligned} \bar{\Omega} + \bar{\omega_\zeta} =& \bar{\Omega} + \bar{\Omega} \left[\frac{3}{2}\frac{e}{R} + \left(q^2 - \frac{3}{2}\frac{e}{R} \right) / \bar{\Omega}^2 \right]^{1/2} \quad \text{high frequency} \\ |\bar{\Omega} - \bar{\omega_\zeta}| =& \left| \bar{\Omega} - \bar{\Omega} \left[\frac{3}{2}\frac{e}{R} + \left(q^2 - \frac{3}{2}\frac{e}{R} \right) / \bar{\Omega}^2 \right]^{1/2} \right| \quad \text{low frequency} \end{aligned} \tag{6.7}$$

Dropping e/R we have

$$\begin{aligned} \bar{\Omega} + \bar{\omega_\zeta} =& \bar{\Omega} + q \quad \text{high frequency} \\ |\bar{\Omega} - \bar{\omega_\zeta}| =& \left| \bar{\Omega} - q \right| \quad \text{low frequency} \end{aligned} \tag{6.8}$$

For $\bar{\Omega} = 0$, the frequencies are $q = \omega_{\zeta 0}/\Omega_0$. The lag frequencies do not change in hover, because unlike flap there is no significant source of aerodynamic damping in lag. Characteristic trends for the fixed frame lag frequencies are shown in Fig. 6.3(a). Figure 6.3(b) shows the typical trends in flap and lag damping.

6.3.3 Rotor Flap and Body Pitch

Three DOF system: β_{1c}, β_{1s}, and θ.
Six roots:

2 zero frequency real roots.
1 pair of complex conjugate high frequency flap.
1 pair complex conjugate low frequency flap-pitch coupled modes.

Figure 6.4 shows the two pairs of complex conjugate roots in vacuum. The dashed lines are the isolated flap frequencies. The plots correspond to $K_y^2 = 0.1$, $p = 1.1$/rev. Figure 6.5 shows the same frequencies in air $\gamma = 5$. Again, the dashed lines are the isolated flap frequencies. The pair of low frequency pitch-flap modes degenerate into 2 unequal real roots with increase in rotational speed before becoming oscillatory again.

6.3.4 Rotor Flap and Body Pitch and Roll

Four DOF system: β_{1c}, β_{1s}, θ, and ϕ.
Eight roots:

2 zero frequency real roots.
1 pair of complex conjugate high frequency flap.

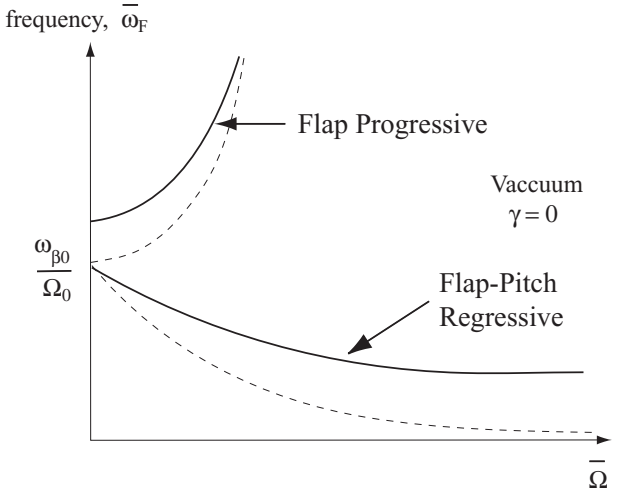

Figure 6.4: **Coupled Flap and Body Pitch Frequencies in Vaccuum**

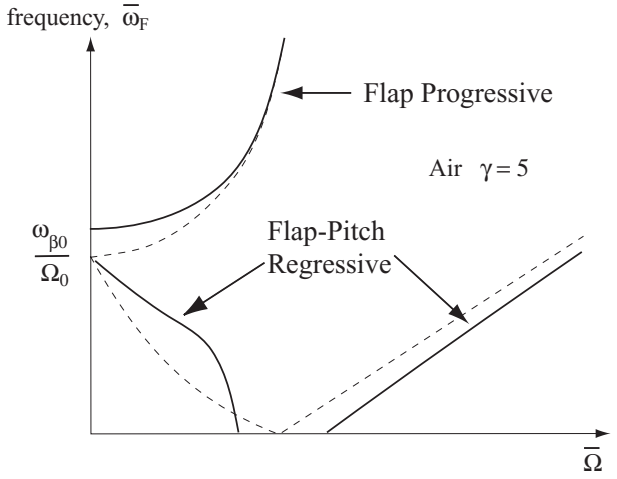

Figure 6.5: **Coupled Flap and Body Pitch Frequencies in Air**

2 pairs of complex conjugate coupled low frequency flap-pitch-gyroscopic modes.
Figure 6.6 shows the frequencies of the three oscillatory complex conjugate modes for the values $K_x^2 = 0.025$, $K_y^2 = 0.1$, and $p = 1.1$/rev. The uncoupled roll and pitch frequencies (non-rotating) are simply due to the fuselage inertia reacting against the blade flap springs. The expressions given in the figure correspond to a four bladed rotor. Figure 6.7 shows the same frequencies including aerodynamic forces in hover for Lock number $\gamma = 5$.

6.3.5 Rotor Flap and Lag and Body Pitch in Vacuum

To avoid confusion with blade pitch angle during the derivation of aerodynamic forces, the body pitch angle will be denoted henceforth as α_y.

Blade Equations

Rotating frame:

$$\overset{**}{\beta} - 2\beta_0 \overset{*}{\zeta} + \nu_\beta^2 \beta - \overset{**}{\alpha}_y \cos\psi + 2 \overset{*}{\alpha}_y \sin\psi = 0$$

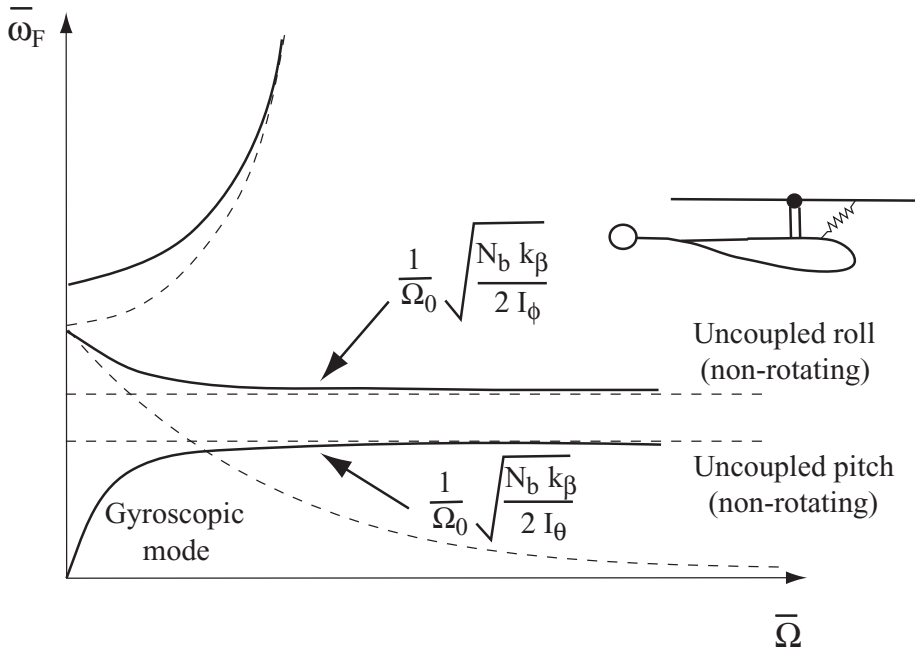

Figure 6.6: **Coupled Flap Body Pitch Roll Frequencies in Vaccuum**

$$\overset{**}{\zeta} + 2\beta_0 \overset{*}{\beta} + g_L \overset{*}{\zeta} + \nu_\beta^2 \zeta + \overset{*}{S}_\zeta \frac{h}{R} \overset{**}{\alpha}_y \sin\psi = 0$$

where h is hub center above body cg.
Fixed Frame:

$$\beta_{1c} : \overset{**}{\beta}_{1c} + 2 \overset{*}{\beta}_{1s} - \beta_{1c} - 2\beta_0(\overset{*}{\zeta}_{1c} + \zeta_{1s}) + \nu_\beta^2 \beta_{1c} - \overset{**}{\alpha}_y = 0$$

$$\beta_{1s} : \overset{**}{\beta}_{1s} - 2 \overset{*}{\beta}_{1c} - \beta_{1s} - 2\beta_0(\overset{*}{\zeta}_{1s} + \zeta_{1c}) + \nu_\beta^2 \beta_{1s} + 2 \overset{**}{\alpha}_y = 0$$

$$\zeta_{1c} : \overset{**}{\zeta}_{1c} + 2 \overset{*}{\zeta}_{1s} - \zeta_{1c} + 2\beta_0(\overset{*}{\beta}_{1c} + \beta_{1s}) + g_L(\overset{*}{\zeta}_{1c} + \zeta_{1s}) + \nu_\zeta^2 \zeta_{1c} = 0$$

$$\zeta_{1s} : \overset{**}{\zeta}_{1s} - 2 \overset{*}{\zeta}_{1c} - \zeta_{1c} + 2\beta_0(\overset{*}{\zeta}_{1s} - \zeta_{1c}) + g_L(\overset{*}{\zeta}_{1s} + \zeta_{1c}) + \nu_\zeta^2 \zeta_{1s} + \overset{*}{S}_\zeta \frac{h}{R} \overset{**}{\alpha}_y = 0$$

Body Equation

$$I_y \ddot{\alpha}_y + c_y \dot{\alpha}_y + K_y \alpha_y = M_y + hH$$

I_y is pitch inertia and c_y is the pitch damping coefficient. M_y is the rotor pitch moment and H is the rotor drag force.

$$M_y = -\sum_{m=1}^{N} M_\beta \cos\psi_m$$

M_b = flap moment at root

$$= -\int_0^R r(m\, dr) r(\ddot{\beta} - \ddot{alpha}_y \cos\psi_m - 2\beta_0 \Omega \dot{\zeta} + 2\Omega \dot{\alpha}_y \sin\psi_m + \Omega^2 \beta)$$

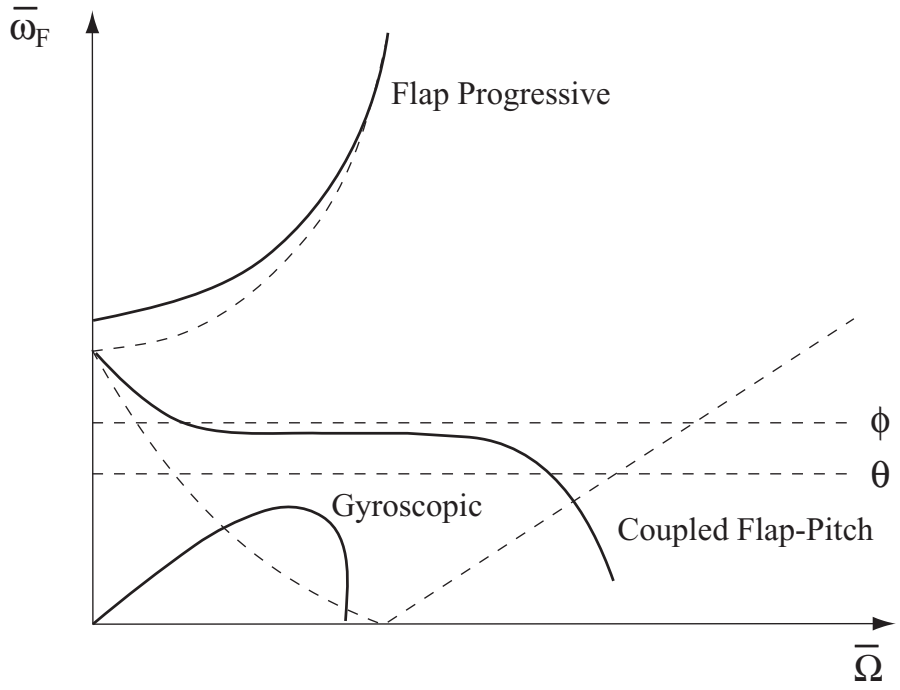

Figure 6.7: **Coupled Flap Body Pitch Roll Frequencies in Air**

$$= -I_b\Omega^2(\overset{*}{\beta} - \overset{**}{\alpha}_y \cos\psi_m - 2\beta_0 \overset{*}{\zeta} + 2 \overset{*}{\alpha} \sin\psi_m + \beta)$$

Radial shear:

$$S_R = -2\Omega \overset{*}{\zeta} \int_0^R mr\, dr - h\ddot{\alpha}_y \cos\psi_m \int_0^R m\, dr$$

$$= -2S_\zeta \Omega \overset{*}{\zeta} - hM_b\ddot{\alpha}_y \cos\psi_m$$

where M_b is blade mass.

Inplane shear:

$$S_x = -(\ddot{\zeta} - \Omega^2\zeta) \int_0^R mr\, dr - h\ddot{\alpha}_y \sin\psi_m \int_0^R m\, dr$$

$$= -(\ddot{\zeta} - \Omega^2\zeta)S_\zeta - hM_b\ddot{\alpha}_y \sin\psi_m$$

Hub drag force:

$$H = \sum^N (S_r \cos\psi_m + S_x \sin\psi_m)$$

$$= \sum^M (-2S_\zeta\Omega\dot{\zeta} \cos\psi_m - hM_b\ddot{\alpha}_y - \ddot{\zeta}S_\zeta \sin\psi_m + \Omega^2\zeta S_\zeta \sin\psi_m)$$

$$= -hM_b\ddot{\alpha}_y - S_\zeta \frac{N}{2} \overset{**}{\zeta}_{1s} \Omega^2$$

$$M_y = I_b\Omega^2 \sum_{m=1}^{N} (\overset{**(m)}{\beta} - \overset{**}{\alpha} \cos\psi_m - 2\beta_0 \overset{*(m)}{\zeta} + 2 \overset{*}{\alpha}_y \sin\psi_m + \beta) \cos\psi_m + hH$$

$$= I_b\Omega^2\frac{N}{2}[\overset{**}{\beta}_{1c} + 2\overset{*}{\beta}_{1s} - \overset{**}{\alpha}_y - 2\beta_0(\overset{*}{\zeta}_{1c} + \zeta_{1s})]$$

Body equation becomes (setting $c_y = K_y = 0$)

$$\overset{**}{\alpha}_y\,(I_y + \frac{NI_b}{2} + Nh^2M_b) - (\overset{**}{\beta}_{1c} + 2\overset{*}{\beta}_{1s} - 2\beta_0\overset{*}{\zeta}_{1c} - 2\beta_0\zeta_{1s})(I_b\frac{N}{2}) + S_\zeta h\frac{N}{2}\overset{**}{\zeta}_{1s} = hH$$

Setting $\overset{*}{I}_y = (I_y + \frac{NI_b}{2} + Nh^2M_b)/\frac{NI_b}{2}$

Body equation becomes

$$\overset{*}{I}_y\overset{**}{\alpha}_y - \overset{**}{\beta}_{1c} - 2\overset{*}{\beta}_{1s} + 2\beta_0\overset{*}{\zeta}_{1c} + 2\beta_0\zeta_{1s} + \overset{*}{S}_\zeta\frac{h}{R}\overset{**}{\zeta}_{1s} = 0$$

Rotor/Body Equations:

$$\begin{bmatrix} 1 & 0 & 0 & 0 & -1 \\ 0 & 1 & 0 & 0 & 0 \\ 0 & 0 & 1 & 0 & 0 \\ 0 & 0 & 0 & 1 & \overset{*}{S}_\zeta\frac{h}{R} \\ -1 & 0 & 0 & \overset{*}{S}_\zeta\frac{h}{R} & \overset{*}{I}_y \end{bmatrix} \begin{Bmatrix} \overset{**}{\beta}_{1c} \\ \overset{**}{\beta}_{1s} \\ \overset{**}{\zeta}_{1c} \\ \overset{**}{\zeta}_{1s} \\ \overset{**}{\alpha}_y \end{Bmatrix}$$

$$+ \begin{bmatrix} 0 & 2 & -2\beta_0 & 0 & 0 \\ -2 & 0 & 0 - 2\beta_0 & 2 & \\ 2\beta_0 & 0 & g_L & 2 & 2\beta_0 \\ 0 & 2\beta_0 & -2 & g_L & 0 \\ 0 & -2 & 2\beta_0 & 0 & 0 \end{bmatrix} \begin{Bmatrix} \overset{*}{\beta}_{1c} \\ \overset{*}{\beta}_{1s} \\ \overset{*}{\zeta}_{1c} \\ \overset{*}{\zeta}_{1s} \\ \overset{*}{\alpha}_y \end{Bmatrix}$$

$$+ \begin{bmatrix} \nu_\beta^2 - 1 & 0 & 0 & -2\beta_0 & 0 \\ 0 & \nu_\beta^2 - 1 & 2\beta_0 & 0 & 0 \\ 0 & 2\beta_0 & \nu_\zeta^2 - 1 & g_L & 0 \\ -2\beta_0 & 0 & -g_L & \nu_\zeta^2 - 1 & 0 \\ 0 & 0 & 0 & 0 & 0 \end{bmatrix} \begin{Bmatrix} \beta_{1c} \\ \beta_{1s} \\ \zeta_{1c} \\ \zeta_{1s} \\ \alpha_y \end{Bmatrix} = 0$$

6.3.6 Rotor Flap and Lag coupled to Body Pitch and Roll in Air

Six DOF system: β_{1c}, β_{1s}, ζ_{1c}, ζ_{1s}, θ, and ϕ.
The body pitch and roll angles θ, and ϕ are henceforth denoted by α_y and α_x to avoid confusion with blade pitch angle.
Twelve roots:

2 zero frequency real roots.

5 complex conjugate pairs: 2 pairs corresponding to β_{1c}, β_{1s}; 2 pairs for ζ_{1c}, ζ_{1s}; and 1 pair for α_y and α_x (the other two roots of the fuselage modes are real).

Figure 6.8 shows the frequencies of the five oscillatory roots. The regressive lag mode has the danger of coalescing with two modes: the regressive flap coupled body pitch-roll and the regressive

flap coupled gyroscopic nutation mode. When it does, it produces air resonance. The damping in regressive lag mode is shown in the bottom diagram. The character of the two regressive flap coupled body modes changes with collective angle, hence the thrust level. For example, figure 6.9 shows the same frequencies at an collective pitch angle of 10^o. The damping of the regressive lag mode becomes further negative, increasing air resonance instability.

$$\begin{bmatrix} 1 & 0 & 0 & 0 & 0 & -1 \\ 0 & 1 & 0 & 0 & 1 & 0 \\ 0 & 0 & 1 & 0 & \overset{*}{S}_\zeta \frac{h}{r} & 0 \\ 0 & 0 & 0 & 1 & 0 & \overset{*}{S}_\zeta \frac{h}{r} \\ 0 & -1 & \overset{*}{S}_\zeta \frac{h}{r} & 0 & \overset{*}{I}_x & 0 \\ -1 & 0 & 0 & \overset{*}{S}_\zeta \frac{h}{r} & 0 & \overset{*}{I}_y \end{bmatrix} \begin{Bmatrix} \overset{**}{\beta}_{1c} \\ \overset{**}{\beta}_{1s} \\ \overset{**}{\zeta}_{1c} \\ \overset{**}{\zeta}_{1s} \\ \overset{**}{\alpha}_x \\ \overset{**}{\alpha}_y \end{Bmatrix}$$

$$+ \begin{bmatrix} 0 & 2 & -2\beta_0 & 0 & 2 & 0 \\ -2 & 0 & 0 & -2\beta_0 & 0 & 2 \\ 2\beta_0 & 0 & g_L & 2 & 0 & 2\beta_0 \\ 2\beta_0 & 0 & g_L & 2 & 0 & 2\beta_0 \\ 0 & 2\beta_0 & -2 & g_L & -2\beta_0 & 0 \\ 2 & 0 & 0 & -2\beta_0 & 0 & 2 \\ 0 & -2 & 2\beta_0 & 0 & -2 & 0 \end{bmatrix} \begin{Bmatrix} \overset{*}{\beta}_{1c} \\ \overset{*}{\beta}_{1s} \\ \overset{*}{\zeta}_{1c} \\ \overset{*}{\zeta}_{1s} \\ \overset{*}{\alpha}_x \\ \overset{*}{\alpha}_y \end{Bmatrix}$$

$$+ \begin{bmatrix} \nu_\beta^2 - 1 & 0 & 0 - 2\beta_0 & 0 & 0 & \\ 0 & \nu_\beta^2 - 1 & 2\beta_0 & 0 & 0 & 0 \\ 0 & 2\beta_0 & \nu_\zeta^2 - 1 & g_L & 0 & 0 \\ -2\beta_0 & 0 & g_L & \nu_\zeta^2 - 1 & 0 & 0 \\ 0 & 0 & 0 & 0 & 0 & 0 \\ 0 & 0 & 0 & 0 & 0 & 0 \end{bmatrix} \begin{Bmatrix} \beta_{1c} \\ \beta_{1s} \\ \zeta_{1c} \\ \zeta_{1s} \\ \alpha_x \\ \alpha_y \end{Bmatrix} = \gamma \begin{Bmatrix} \overline{M}_{\beta_{1c}} \\ \overline{M}_{\beta_{1s}} \\ \overline{M}_{\zeta_{1c}} \\ \overline{M}_{\zeta_{1s}} \\ \overline{c}_{mx} \\ \overline{c}_{my} \end{Bmatrix}$$

Aerodynamic forces are broken into stiffness and damping contributions.

$$\gamma \begin{Bmatrix} \overline{M}_{\beta_{1c}} \\ \overline{M}_{\beta_{1s}} \\ \overline{M}_{\zeta_{1c}} \\ \overline{M}_{\zeta_{1s}} \\ \overline{c}_{mx} \\ \overline{c}_{my} \end{Bmatrix} = K_A \begin{Bmatrix} \beta_{1c} \\ \beta_{1s} \\ \zeta_{1c} \\ \zeta_{1s} \\ \alpha_x \\ \alpha_y \end{Bmatrix} + C_A \begin{Bmatrix} \overset{*}{\beta}_{1c} \\ \overset{*}{\beta}_{1s} \\ \overset{*}{\zeta}_{1c} \\ \overset{*}{\zeta}_{1s} \\ \overset{*}{\alpha}_x \\ \overset{*}{\alpha}_y \end{Bmatrix}$$

where the components of K_A and C_A are as follows.

$$
K_A = \gamma \begin{bmatrix}
\frac{\gamma}{8}\kappa_{p\beta} & \frac{\gamma}{8} & \frac{\gamma}{8}\kappa_{p\zeta} & \gamma(\frac{\theta}{4}-\frac{\lambda}{6}) & 0 & 0 \\
-\frac{\gamma}{8} & \frac{\gamma}{8}\kappa_{p\beta} & -\gamma(\frac{\theta}{4}-\frac{\lambda}{6}) & \frac{\gamma}{8}\kappa_{p\zeta} & 0 & 0 \\
\frac{\gamma}{6}(\lambda\kappa_{p\beta}) & -\gamma(\frac{\theta}{8}-\frac{\lambda}{3}) & \frac{\gamma}{6}(\lambda\kappa_{p\zeta}) & \frac{\gamma}{8}(\frac{2c_d}{a}) & 0 & 0 \\
 & \gamma(\frac{\theta}{8}-\frac{\lambda}{3})\frac{\gamma}{6}(\lambda\kappa_{p\beta}) & -\frac{\gamma}{8}(\frac{2c_d}{a}) & \frac{\gamma}{6}(\lambda\kappa_{p\zeta}) & 0 & 0 \\
-\frac{\gamma}{8}+\frac{\gamma\overline{h}}{2}(\frac{\beta}{3}+\frac{\lambda\kappa_{p\beta}}{4}) & (\frac{\gamma}{8}-\frac{\beta\gamma\overline{h}}{6})\kappa_{p\beta}-\frac{\gamma\overline{h}}{2}(\frac{\theta}{3}-\lambda) & -\gamma(\frac{\theta}{4}-\frac{\lambda}{6})+\gamma\overline{h}\beta(\frac{\theta}{3}-\frac{\lambda}{4})+\frac{\lambda\gamma\overline{h}}{4}\kappa_{p\zeta} & \kappa_{\rho\zeta}(\frac{\gamma}{8}-\frac{\beta\gamma\overline{h}}{6})+\frac{\gamma\overline{h}}{6}(\frac{2c_d}{a}) & 0 & 0 \\
-(\frac{\gamma}{8}-\frac{\beta\gamma\overline{h}}{6})\kappa_{p\beta}+\frac{\gamma\overline{h}}{2}(\frac{\theta}{3}-\lambda) & -\frac{\gamma}{8}+\frac{\gamma\overline{h}}{2}(\frac{\beta}{3}+\frac{\lambda\kappa_{p\beta}}{4}) & -\kappa_{\rho\zeta}(\frac{\gamma}{8}-\frac{\beta\gamma\overline{h}}{6})-\frac{\gamma\overline{h}}{6}(\frac{2c_d}{a}) & -\gamma(\frac{\theta}{4}-\frac{\lambda}{6})+\gamma\overline{h}\beta(\frac{\theta}{3}-\frac{\lambda}{4})+\frac{\lambda\gamma\overline{h}}{4}\kappa_{\rho\zeta} & 0 & 0
\end{bmatrix}
$$

$$
C_A = \gamma \begin{bmatrix}
\frac{\gamma}{8} & 0 & \gamma(\frac{\theta}{4}-\frac{\lambda}{6}) & 0 & \gamma\overline{h}(\frac{\theta}{3}-\frac{\lambda}{4}) & -\frac{\gamma}{8} \\
0 & \frac{\gamma}{8} & 0 & \gamma(\frac{\theta}{4}-\frac{\lambda}{6}) & \frac{\gamma}{8} & \gamma\overline{h}(\frac{\theta}{3}-\frac{\lambda}{4}) \\
-\gamma(\frac{\theta}{8}+\frac{\lambda}{3}) & 0 & \frac{\gamma}{8}(\frac{2c_d}{a}) & 0 & \frac{\gamma\overline{h}}{6}(\frac{2c_d}{a}) & \frac{\gamma\theta}{8} \\
0 & -\gamma(\frac{\theta}{8}+\frac{\lambda}{3}) & 0 & \frac{\gamma}{8}(\frac{2c_d}{a}) & \frac{\gamma\theta}{8} & \frac{\gamma\overline{h}}{6}(\frac{2c_d}{a}) \\
\gamma\overline{h}(\frac{\theta}{6}-\frac{\lambda}{2}) & \frac{\gamma}{8}-\frac{\gamma\overline{h}\beta_0}{6} & \frac{\gamma\overline{h}}{6}(\frac{c_d}{a}) & \gamma(\frac{\theta}{4}-\frac{\lambda}{6})-\gamma\overline{h}(\frac{\theta\beta}{3}-\frac{\lambda\beta}{4}) & \frac{\gamma}{8}-\frac{\gamma\overline{h}\beta}{6}+\frac{\gamma\overline{h}^2}{4}(\frac{c_d}{a}) & \gamma\overline{h}(\frac{\theta}{2}-\frac{\lambda}{4})-\gamma\overline{h}^2(\frac{\theta\beta}{2}-\frac{\lambda\beta}{4}) \\
-(\frac{\gamma}{8}-\frac{\gamma\overline{h}\beta_0}{6}) & -\gamma\overline{h}(\frac{\theta}{6}-\frac{\lambda}{2}) & -\gamma(\frac{\theta}{4}-\frac{\lambda}{6})+\gamma\overline{h}(\frac{\theta\beta}{3}-\frac{\lambda\beta}{4}) & \frac{\gamma\overline{h}}{6}(\frac{2c_d}{a}) & -\gamma\overline{h}(\frac{\theta}{2}-\frac{\lambda}{4})+\gamma\overline{h}^2(\frac{\theta\beta}{2}-\frac{\lambda\beta}{2}) & \frac{\gamma}{8}-\frac{\gamma\overline{h}\beta}{6}+\frac{\gamma\overline{h}^2}{4}(\frac{c_d}{a})
\end{bmatrix}
$$

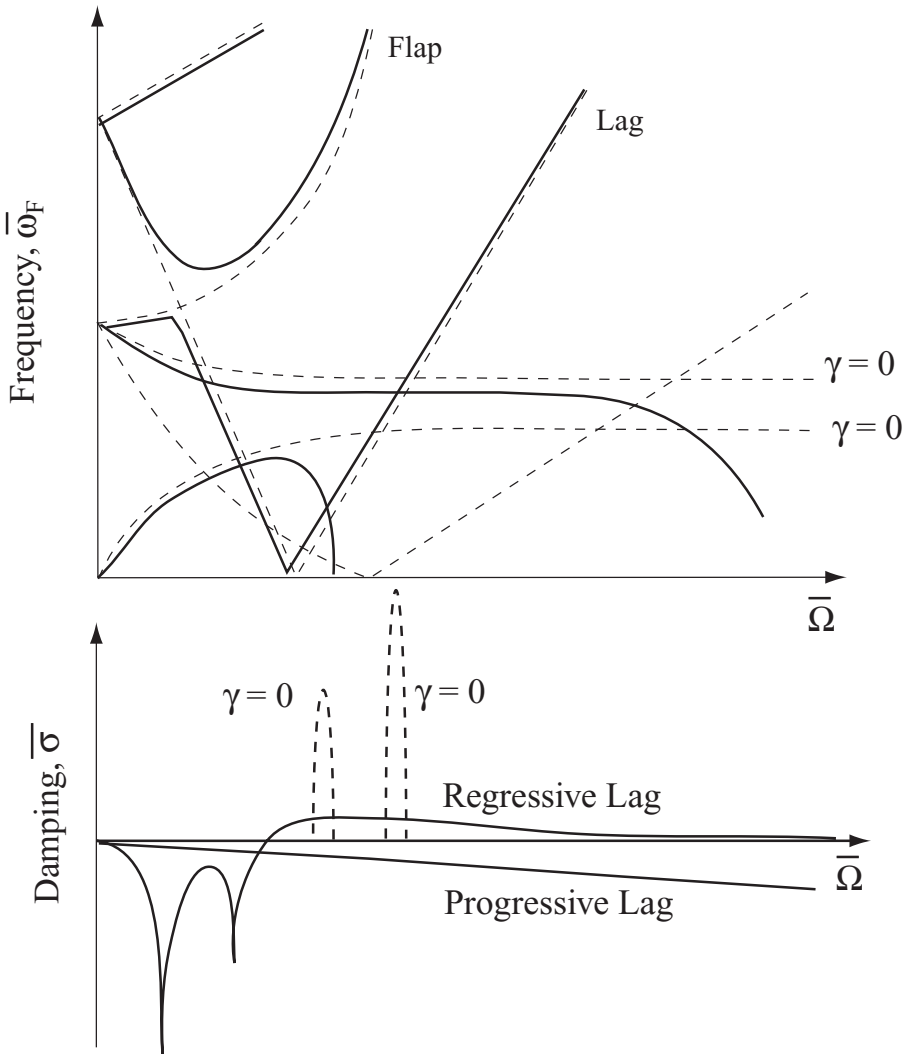

Figure 6.8: **Coupled Flap, Lag, Pitch, Roll Air-Resonance Modes; Collective angle = 0^o**

6.4 Experimental Data on Aeromechanical Stability

A comprehensive experimental test program to measure the aeromechanical stability of a hingeless rotor was undertaken by Bousman [3]. The model was a 1.62-m diameter, three-bladed rotor mounted on a static mast. The mast was bolted to a transmission and two electric drive motors, together constituting the model. The model was supported on a gimballed frame which allowed pitch and roll motions. The blades were rigid with flexibility concentrated at the root end flexures. The flexures created virtual lag and flap hinges. From the center of the hub, the lag hinge flexure was located inboard, followed by the flap hinge flexure outboard. When assembled, the flap and lag hinge were coincident. The lag stiffness was greater than the flap stiffness, as in conventional rotors. The flexure representing the lag hinge could be substituted with a skewed flexure to produce negative pitch lag coupling of $K_{p\zeta} = -0.4$. The flexure representing the flap hinge could be substituted with another with eight times the stiffness to produce the same non-rotating flap and lead-lag frequencies were equal with the blade set at zero pitch angle. The blade pitch angle could be changed manually, either outboard or inboard of the flexures. Five configurations were tested. They are given in table 6.1.

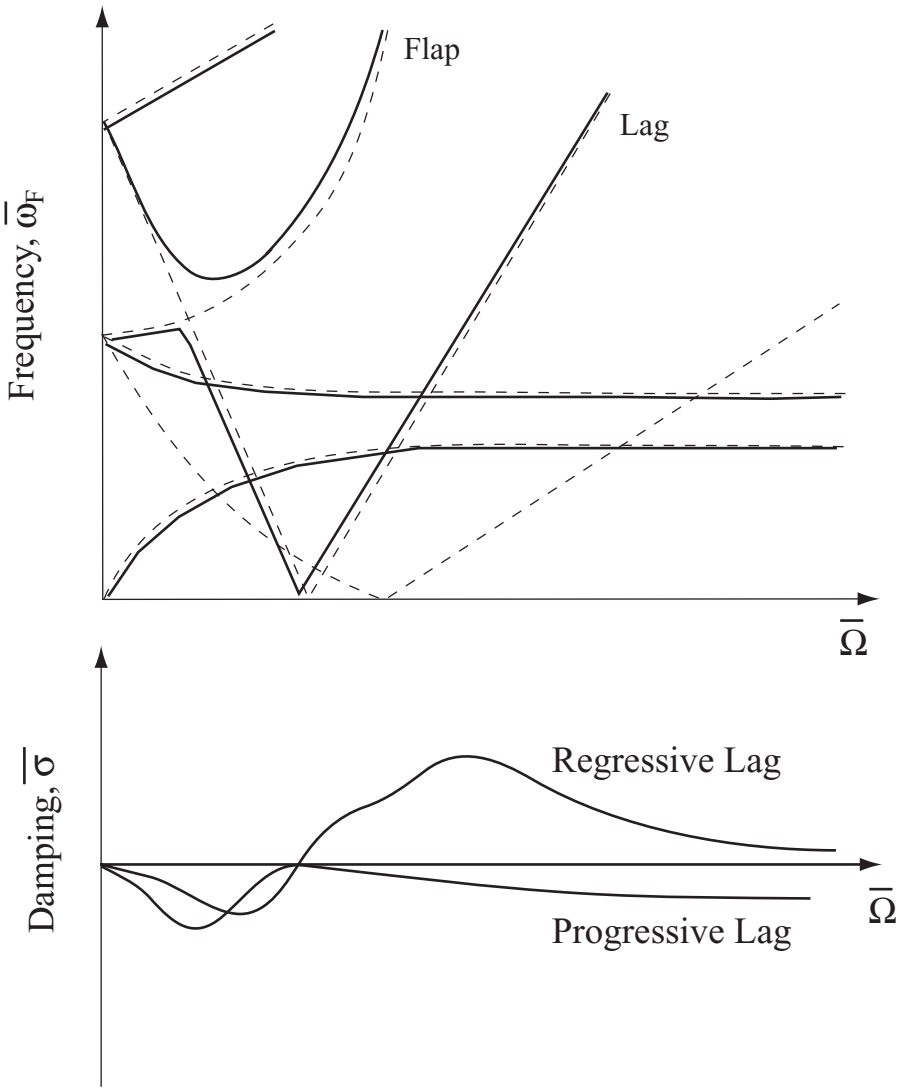

Figure 6.9: **Coupled Flap, Lag, Pitch, Roll Air-Resonance Modes; Collective angle = 10^o**

The nominal rotor speed was 720 rpm. The rotor dimensionless lead-lag frequency at this rpm was 0.70/rev. The low frequency lead-lag regressing mode in the fixed coordinates was therefore at 0.30/rev. The body frequencies were controlled by cantilevered springs mounted across the gimbal flexural pivots. The springs were selected to provide body pitch and roll frequencies of 0.12/rev and 0.28/rev (2 Hz and 4 Hz at 720 rpm). The pitch mode is lower than the lead-lag regressive mode, while the roll mode is quite close and represents a critical design condition. The placement of frequencies was representative of air resonance conditions for a number of full-scale soft inplane rotor helicopters [4, 5, 6, 7]. The structural properties are given in table 6.2.

The blade properties are mean of three blades. The blade frequency and percentage critical damping are given in table 6.3. The structural properties of the body are given in table 6.4.

The gimbal frame acted as a part of the body during pitch motions, hence the difference in mass and c.g. location in pitch and roll. The vertical c.g. location is above the gimbal plane. The rotor disk was 24.10 cm above the gimbal plane. The body pitch and roll mode damping in terms of percentage critical were

$$\xi_\alpha = 3.200\% \quad \xi_\phi = 0.929\%$$